The Role of Ocean Dynamics for Low-Frequency Fluctuations of the NAO in a Coupled Ocean–Atmosphere GCM

M. CHRISTOPH

Max-Planck-Institut für Meteorologie, Hamburg, Germany

U. ULBRICH

Institut für Geophysik und Meteorologie, Universität zu Köln, Cologne, Germany

J. M. OBERHUBER

Deutsches Klimarechenzentrum, Hamburg, Germany

E. ROECKNER

Max-Planck-Institut für Meteorologie, Hamburg, Germany

(Manuscript received 11 January 1999, in final form 14 July 1999)

ABSTRACT

Variability at all timescales, including low-frequency variability, is found in the North Atlantic sector in a 300-yr control integration of the coupled ocean–atmosphere general circulation model (CGCM) ECHAM4/OPYC3. The atmospheric variability is dominated by the North Atlantic Oscillation (NAO). Only rather weak spectral peaks are superimposed on the ''white noise'' power spectrum of sea level pressure and on the essentially ''red noise'' spectrum of SST in highly active regions. Replacing the full ocean model with a 50-m fixed-depth mixed layer ocean (MLO) and coupling it to the atmosphere yields qualitatively and quantitatively very similar power spectra of the NAO index.

Net surface heat fluxes, describing the coupling between the ocean and the atmosphere for the long-term variations (>10 yr) of the NAO are much weaker in the MLO model, but show general agreement in both simulations regarding spatial distributions. This spatial agreement with respect to NAO variability occurs even though the associated SST anomaly pattern in the CGCM is shifted northward by about 10° relative to its position in the run without the dynamical ocean. This fact is mainly attributed to advection in the full ocean model.

There is evidence for the existence of ocean–cryosphere–atmosphere coupling in the CGCM. From the fact that we found only weak spectral peaks it appears that the role of a fully coupled ocean with respect to long-term NAO variability is limited to a shift in SST variability and to a moderate increase of the atmosphere's long-term variability over most part of the domain. In view of the subordinate relevance of ocean–atmosphere coupling for the NAO it is suggested that the CGCM presented in this study mainly follows the stochastic climate model concept, that is, the ocean integrates over the chaotic forcing imposed by the atmosphere, leaving the NAO rather unpredictable on decadal and longer timescales.

1. Introduction

The low-frequency variability of the North Atlantic oscillation (NAO) has recently become one of the foci of climate research (CLIVAR 1998). This is partly due to the desire to perform long-range predictions for the European area where climate variability is strongly influenced by this feature (Wanner et al. 1997). Numerous observational studies have given evidence that NAO variability exists basically on all timescales, including those of a decade and longer (Rogers 1984, 1990; Hurrell 1995; Hurrell and van Loon 1997; Rogers 1997; Schmutz and Wanner 1998). On interannual timescales it seems to be mainly the chaotic behavior of the extratropical atmosphere that is forcing red noise characteristics of the ocean locally (Kushnir 1994; Saravanan 1998). Recent modeling studies, however, pointed to a possible indirect influence of surface boundary conditions on the atmospheric circulation via the storm track (Palmer and Sun 1985; Ferranti et al. 1994; Bresch and Davies 1998). The question of practical NAO predictability has recently been addressed by Rodwell et

Corresponding author address: Dr. Michael Christoph, Institut für Geophysik und Meteorologie, Universität zu Köln, Kerpener Str. 13, D-50923 Cologne, Germany.
E-mail: christoph@meteo.uni-koln.de

al. (1999) using a set of runs with an atmospheric GCM (AGCM) and observed SSTs. They find that the low-frequency part of the observed NAO time series is roughly reproduced by the ensemble mean of these runs during the second part of this century. The authors conclude that oceanic influence on the atmosphere is not negligable for this part of atmospheric variability.

Still highly under debate are the mechanisms of low-frequency fluctuations. We note that in many observational studies the ocean is attributed a crucial role in this process. For instance, Deser and Blackmon (1993) suggest the existence of two major modes of SST variability: a wind-driven dipole pattern operating both on quasi-biennial and quasi-decadal timescales and an ocean-driven monopole centered along the Gulf Stream. Kushnir (1994) presents evidence for the existence of an interdecadal and basin-scale SST mode. It is of one polarity and possesses a nonlocal relationship with the overlying atmosphere in opposition to the interannual mode. Encouraging results regarding the prospects of decadal predictability has been given by Sutton and Allen (1997). They find SST anomalies to appear and propagate along the path of the Gulf Stream with a period of about 12 yr. However, the shortness and incompleteness of marine and aerial records available today are responsible for the fact that the origin of observed modes still remains obscure.

Multicentury GCM experiments have enabled the development of several hypotheses explaining long-term variability in the atmosphere and the ocean. The simplest one consists of the concept of a stochastic climate model (Hasselmann 1976), where the ocean integrates over the high-frequency forcing of the atmosphere. This concept has been suggested to be applicable also on decadal and longer timescales (Manabe and Stouffer 1996; Halliwell 1997). The stochastic climate model, however, can explain only the redness of climate spectra but not the existence of dominant spectral peaks. Coupling between the ocean and the atmosphere is suggested to generate damped eigen-oscillations at rather well-defined frequencies that are superimposed on the background noise (Latif and Barnett 1994; Frankignoul et al. 1997). Over the North Atlantic, for instance, the atmospheric component of such coupled modes seems to be reflected by a typical NAO pattern. The long-term memory of coupled systems is suggested to reside in the ocean due to its large inertia. Crucial memory elements in the North Atlantic section were proposed to consist of low-frequency variations of the gyral circulation (Grötzner et al. 1998; Saravanan and McWilliams 1998; Latif 1998) and/or the thermohaline circulation (Delworth et al. 1993; Saravanan and McWilliams 1997; Timmermann et al. 1998). It seems that simulated processes involving horizontal advection operate preferably on timescales of 1–2 decades, whereas the formation of bottom water appears to be linked mainly with interdecadal variations.

Excitations of coupled eigenmodes are also conceivable between other components of the climate system, such as ocean and cryosphere (Mysak et al. 1990; Yang and Neelin 1993). And finally, another hypothesis consists of a coupling between the stratospheric vortex and the tropospheric circulation, which are proposed to contribute to NAO variability (Perlwitz and Graf 1995). In this case, however, it is still an open question where the memory of the system is to be located.

The main goal of this paper is to assess the role of ocean dynamics for NAO fluctuations on decadal and longer timescales by comparison of a coupled full ocean–atmosphere GCM with a mixed layer ocean–atmosphere GCM. The two models, datasets, and basic methods applied are described in section 2. Subsequently, we compare the spectra of the NAO index produced by these runs in section 3 and the decadal-scale patterns of SST and surface heat flux associated with the NAO in section 4. SST spectra and the existence of some of the recently proposed coupled modes and their importance for the decadal NAO are investigated in section 5.

2. Datasets and methods

The AGCM used in this study is the ECHAM4 developed at the Max Planck Institute for Meteorology in Hamburg. This version of the model has 19 hybrid levels in the vertical extending to 10 hPa and a horizontal resolution of T42 (corresponding to a longitude–latitude grid of about $2.8^\circ \times 2.8^\circ$). A detailed description of the model is found in Roeckner et al. (1996). Coupled to the atmosphere is OPYC3, a full ocean general circulation model (OGCM) posed in isopycnal coordinates with embedded mixed layer and a dynamic–thermodynamic sea-ice model including viscous plastic rheology (Oberhuber 1993a,b). Outside the Tropics the ocean model possesses the same spatial resolution as the atmospheric component, while equatorward of 36° the spacing between latitude circles is gradually decreased to 0.5° in order to resolve the equatorial wave guide and thus realistically simulate ENSO. An annual mean flux correction scheme of heat and freshwater developed by Bacher et al. (1998) is introduced in order to compensate for the difference in fluxes delivered by the AGCM and those requested by the OGCM, whereas wind stress fields remain uncorrected. The flux correction is computed by continuous updating during a 100-yr spinup phase and afterward kept fixed in time for the fully coupled run, hereafter referred to as CGCM.

We investigate a 300-yr control integration for present-day climate conditions. Apart from atmospheric quantities such as sea level pressure (SLP), net surface heat flux, and derived atmospheric quantities such as storm tracks [assessed on a daily basis for each month according to the technique of Christoph et al. (1995)], also parameters taken from the ocean model are considered here such as SST, sea surface salinity, surface velocity, and the strength of the thermohaline circulation (THC) as measured by the meridional overturning

(MOT). Our study focuses on the North Atlantic and north polar sector (90°W–30°E, 20°–88°N) and is restricted to cold season conditions represented by averages from November through March. This latter choice is motivated by the fact that the extratropical atmospheric circulation is weaker in boreal summer than in winter and that low-frequency interactions between ocean and atmosphere are inhibited in the summertime due to a relatively thin and warm mixed layer capping the deeper ocean (Woods 1985; Kushnir 1994). In order to separate high- and low-frequency variability a 10-yr low-pass filter based on fast Fourier transformation (Press et al. 1989) was applied.

For a second multicentury control integration the spectral resolution of the atmosphere was reduced to T30 (corresponds to a grid of about 3.75° lat × 3.75° long) and the AGCM coupled to a mixed layer ocean model, hereafter referred to as MLO. The thermodynamic sea-ice formulation is the same as in the CGCM except for the lack of fractional sea-ice coverage of grid boxes. The MLO lacks an interior ocean, has a fixed-depth mixed layer of 50 m, and is horizontally insulated. In order to obtain a realistic seasonal cycle, monthly means of heat are flux corrected on the basis of the observed climatological cycle of surface temperatures for the period 1979–88. The climatology of the ECHAM4-T30 atmospheric model and many aspects of its variability were shown to be close to the T42 version (Stendel and Roeckner 1998) while at the same time the reduction of computer time is substantial. Time series comprising 390 winter means were compiled for all parameters considered before in the T42 model in an analogous way, except for the dynamic ocean quantities.

Note that a preprocessing procedure was applied to the surface temperature dataset. At water points where the ocean is covered by sea ice the original ice surface temperature value is set to −1.8°C. This is done to avoid contributions from the highly variable ice surface temperature to the total SST variance of the entire North Atlantic.

Empirical orthogonal function (EOF) analysis (Kutzbach 1967; Preisendorfer 1988) is the method we chose for describing variations of a complex geophysical field. This method has become a common procedure in meteorological and oceanographic data analysis since it results in a relatively small number of functions and associated time coefficients. Another advantage lies in the fact that the leading modes often are accessable to physical interpretation thereby giving insight into intricate processes. In cases, however, where the data field contains traveling waves, one has to resort, for instance, to modified EOF techniques such as complex EOFs (Barnett 1983) or extended EOFs (Weare and Nasstrom 1982).

3. Simulated NAO variability

We begin our investigations with the description of atmospheric variability aspects found over the North Atlantic of the CGCM control run. Performance of an EOF analysis of 10-year low-pass-filtered SLP fields yields a dominant north–south-oriented dipole pattern that explains more than 47% of the filtered variance (not shown). This mode can be identified with the well-known NAO according to the high structural agreement with the dominant eigenmode observed in January on the basis of unfiltered German Weather Service data (Glowienka-Hense 1990, her Fig. 2). Further support for the identification of the NAO with the leading EOF is given by the fact that the first principal component (PC) is highly correlated ($r = 0.96$) with an index time series characterizing the pressure seesaw between the Greenland–Iceland area and the lower latitudes over the Atlantic and Mediterranean. Following closely the definition of Hurrell (1995), the index is constructed from the difference of normalized pressures between area averages located just west of Portugal (40°–43°N, 11°–14°W) and over Iceland (65°–68°N, 17°–20°W). Area averages are normalized by division of each winter mean pressure by the respective standard deviation. The selection of the above index regions is motivated by the position of centers of maximum teleconnectivity, that is, of strongest negative correlation [for methodical description see Wallace and Gutzler (1981)]. Positive (negative) index values indicate anomalously strong (weak) geostrophic westerlies over the North Atlantic and northwestern Europe. For reasons of simplicity and in order to make results more comparable with other studies, the NAO index rather than the first PC will be used in this study. The 10-year low-pass-filtered index is plotted in Fig. 1a and marked by the thick solid line. The energy spectrum of the unfiltered index (see Fig. 1a, thin solid line), although essentially characterized by white noise behavior, exhibits two significant peaks, one around 7.5 yr and a second less pronounced one around 30 yr (Fig. 1b).

We also checked to what extent the variability of SLP at grid points used for the CGCM's NAO index is reproduced realistically. This was done by computing the variance of unfiltered SLP during the cold season both from the model and from observations [141 yr (1855–1995) of station data gathered at Lisbon, Portugal, and in southwestern Iceland]. We find $\sigma^2_{\text{Lisbon}} = 4.0$ hPa^2 compared with 5.1 hPa^2 in the model's southern (subtropical) NAO center and $\sigma^2_{\text{Iceland}} = 16.8$ hPa^2 compared with 21 hPa^2 in the model's northern (subpolar) NAO center. Note that differences between observation and simulation are not significant on the 95% confidence level according to an F test. When taking into account only the 10-yr low-pass-filtered part of the spectrum, we again obtain a realistic simulation of the respective variability contributions. In this case the variances read as follows: $\sigma^2_{\text{Lisbon}} = 0.5$ hPa^2 ($\sigma^2_{\text{subtropical}} = 0.5$ hPa^2 in the model) and $\sigma^2_{\text{Iceland}} = 3.6$ hPa^2 ($\sigma^2_{\text{subpolar}} = 2.4$ hPa^2 in the model). Again, differences are not significant. The spectrum of the observed NAO index is slightly red on interannual timescales. Note that it possesses one sig-

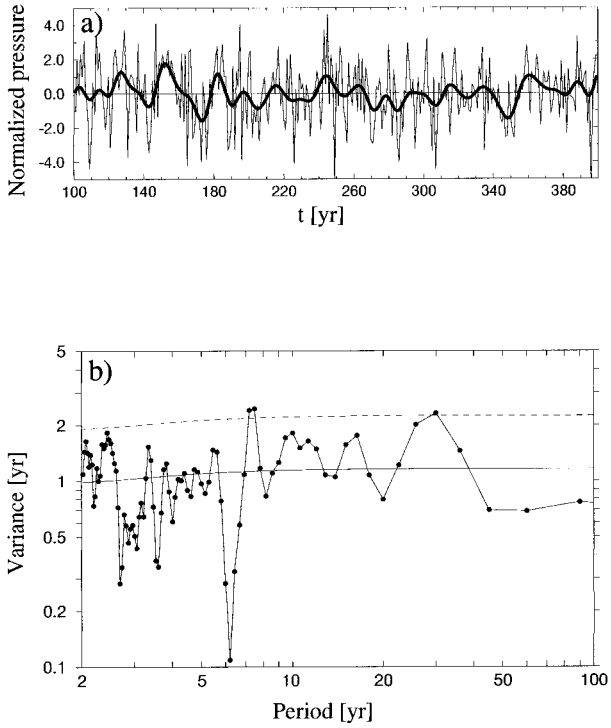

FIG. 1. (a) Unfiltered (thin line) and 10-yr low-pass-filtered (thick line) NAO index (for definition see section 3) time series in winter (Nov–Mar) as simulated by the CGCM. (b) Power spectrum of the unfiltered NAO index. The spectrum is based on a Hanning–Tukey window with a maximum of 90 lags. The solid line denotes the spectrum of an equivalent red noise process and the dashed line denotes the 95% confidence level for accepting the red noise null hypothesis.

nificant peak around 7.5 yr (Fig. 2), that is, at the same frequency found in the CGCM's spectrum (cf. Fig. 1b). Also note that the spectra of Figs. 1b and 2 are quantitatively comparable due to the aforementioned agreement of observed and modelled variances, which enter the definition of the respective NAO index as normalizations.

Analogously we analyzed the integration of the mixed layer model (for model details see section 2) whose ocean only serves as heat storage. Geographical locations of the two activity centers of the NAO are almost identical with those in the CGCM and in the observational data (Glowienka-Hense 1990; Hurrell 1995). The T30-NAO index time series and its energy spectrum are plotted in Figs. 3a and 3b, respectively. The clearly *white* noise power spectrum shows only one significant peak around 2.5 yr. Despite the absence of significant peaks at periods of a decade and longer, there are still nonnegligible energy contributions coming from that part of the spectrum. The variance of the unfiltered SLP time series amounts to $\sigma^2_{\text{subtropical}} = 5.1$ hPa^2 and to $\sigma^2_{\text{subpolar}} = 15.2$ hPa^2. This means a reduction of variability only at the nothern dipole center of approximately 27% compared with the CGCM (significant on the 99% confidence level according to an F test). The

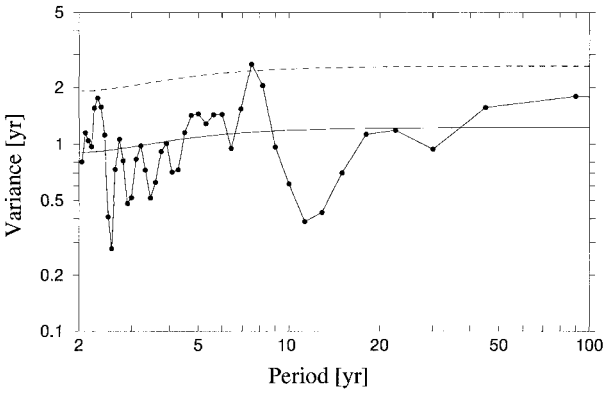

FIG. 2. As in Fig. 1b but for the 141-yr record of observed station data at Lisbon, Portugal, and in southwestern Iceland.

variances of 10-yr low-pass-filtered time series at these two locations read as follows: $\sigma^2_{\text{subtropical}} = 0.6$ hPa^2 and $\sigma^2_{\text{subpolar}} = 2$ hPa^2. Comparing these numbers with those obtained from the CGCM above it turns out that, according to an F test, there is no significant difference in the low-frequency variability of the NAO centers in the absence of a dynamical ocean.

4. Relation between NAO, surface heat flux, and SST

In this section we investigate the connections between the low-frequency atmospheric NAO and the associated

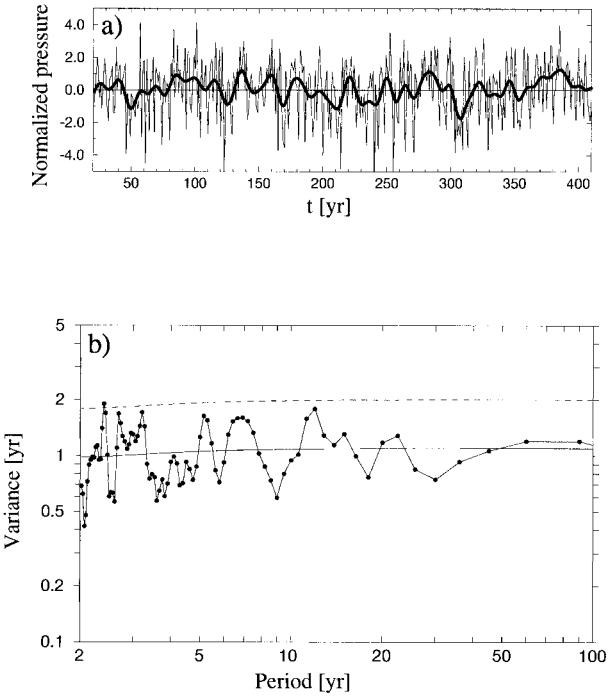

FIG. 3. (a) As in Fig. 1a but for the MLO run. (b) As in Fig. 1b but for the MLO run.

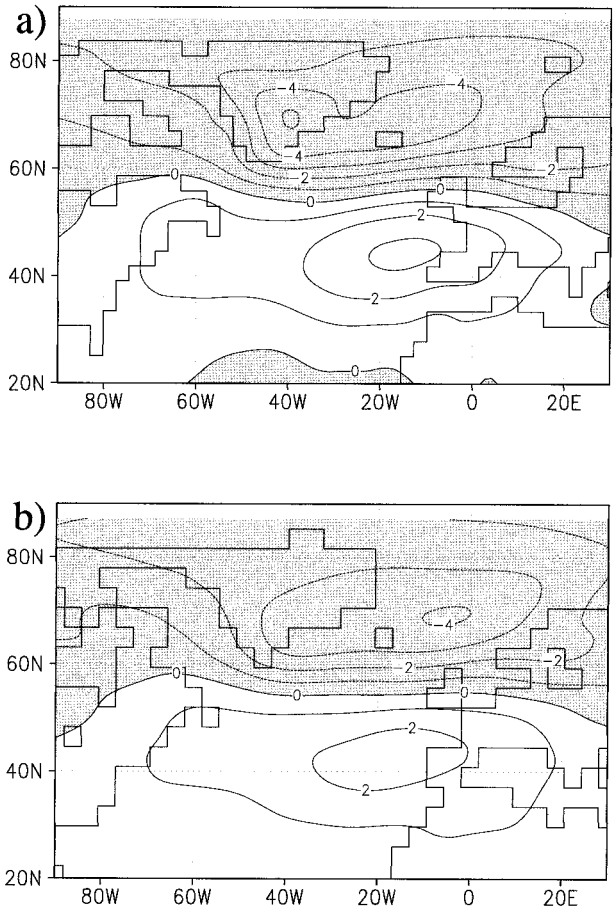

FIG. 4. Decadal NAO composite fields (high index minus low index, threshold being one standard deviation) of sea level pressure (hPa) as simulated by (a) the CGCM (T42) and (b) the MLO (T30). Negative values are shaded.

oceanic variability. As a first approach we consider composite differences between NAO extreme phases. Ensemble members of positive and negative composites are keyed to index values (taken from Fig. 1a, thick solid line) greater and smaller than one standard deviation, respectively. The resulting large-scale anomalies will be discussed in the following text and are all locally significant on the 95% confidence level according to a *t* test.

The anomalous pressure patterns encountered during a positive NAO phase in the CGCM (Fig. 4a) and the MLO run (Fig. 4b) are very similar (spatial correlation coefficient $r_s = 0.96$). In particular, pressure gradients over the North Atlantic are at the same position. At this point we would like to address in more detail the question to what extent the low-frequency variability associated with the NAO in the CGCM is reproduced by the MLO. Since Monte Carlo type simulations of the two models are not available, a different approach has to be chosen. In section 3 it was already shown that there is no significant difference in long-term variability as measured by the variance between respective NAO activity centers. This result, however, could be accidental and may not be true for the entire domain. It turns out that there is a spatially coherent underestimation of variance in the MLO over most part of the North Atlantic sector (not shown). From EOF analysis we know that the first SLP mode of each model run, which is associated with the NAO, explains about equal amounts (47% and 48%) of the domain's total low-frequency variability. Thus, in order to answer the question raised above it is sufficient to know to what extent the total low-frequency variability of SLP is reproduced. We find that it is underestimated by about 15% in the MLO compared with the CGCM. This value is significant on the 99% confidence level and translates into a 15% underestimation of the NAO-related variance on decadal and longer timescales. The overall significance is based on the estimation of an effective degree of freedom, which takes into account not only the 10-yr low-pass filtering of the time series but also an average influence radius of about 1500 km due to correlations with neighboring grid points.

The atmospheric composite anomalies described above are also associated with a large area of negative (upward directed) net surface heat fluxes (equals the sum of surface latent and sensible heat flux, and surface solar and thermal radiation) south of Greenland, mainly due to fluxes of sensible and latent heat (Fig. 5a for the CGCM and Fig. 5b for the MLO). Positive (downward directed) fluxes in the central parts of the North Atlantic are mainly due to anomalous solar radiation. The upward heat flux anomalies are partly the result of cold and dry Arctic air mass advected over the Labrador Sea and also of enhanced westerly surface winds over the northwestern Atlantic. Both processes effectively cool the ocean south of Greenland. The amplitudes of the simulated heat flux anomalies connected with decadal NAO extremes are about four times larger in the CGCM than in the MLO while their spatial distributions are rather similar.

Investigation of the SSTs associated with a positive phase of the NAO shows the following picture. The pattern for the mixed layer ocean (Fig. 6b) has a characteristic dipole structure with negative SST anomalies of up to -1 K to the north and positive SST anomalies of up to $+0.3$ K to the south of 45°N, thus being spatially in phase with the anomalous heat flux pattern of this model (Fig. 5b). For the OPYC (ocean in isopycnal coordinates) (cf. Fig. 6a) the sharp meridional SST gradient in the western North Atlantic is shifted northward by about 10° resulting in a 90° out-of-phase relation between SST and heat flux patterns. This is most likely due to the advective effects of ocean surface currents. During the positive NAO phases they are increased largely around Newfoundland (Fig. 7) leading to enhanced northward transports of warm waters from the subtropics along the east coast of North America. This increase amounts to about 5% with respect to the cli-

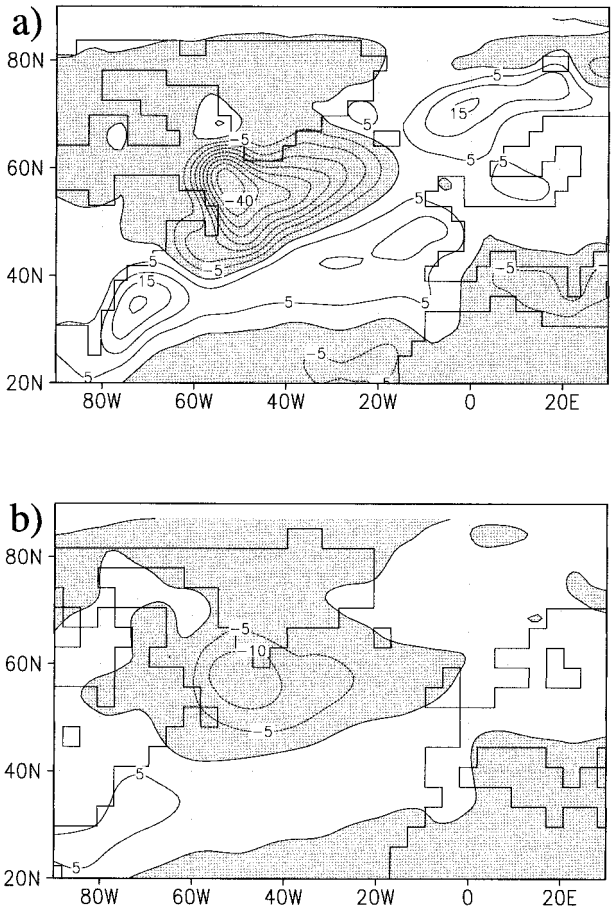

FIG. 5. As in Fig. 4 but for net surface heat flux (W m^{-2}).

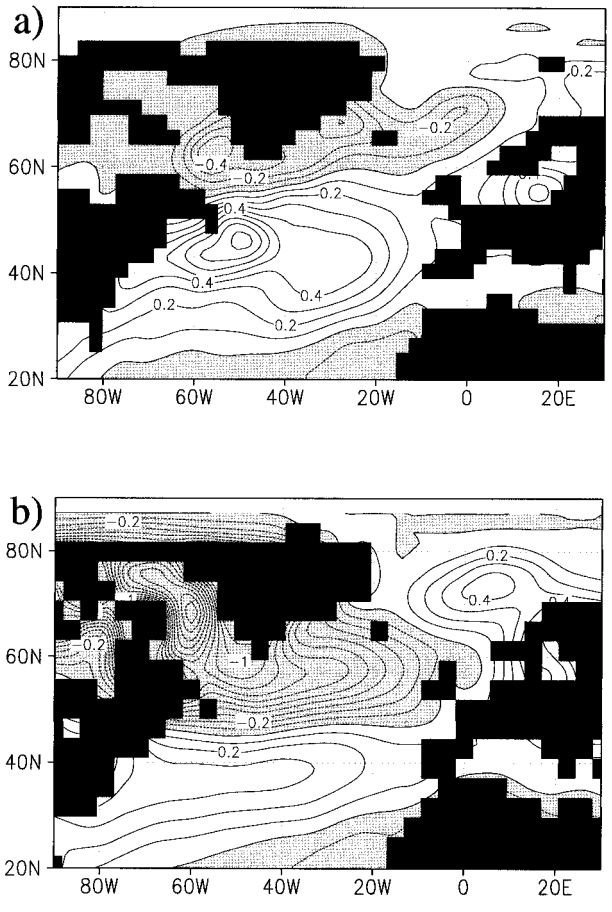

FIG. 6. As in Fig. 4 but for SST (K).

matological mean surface velocity. Additional dynamical processes could also contribute to the aforementioned out-of-phase relationship between heat fluxes and SSTs, such as (i) increased heat flux into the ocean in the subtropics effecting a higher heat content of the Gulf Stream or (ii) increased vertical mixing in the upper ocean due to stronger wind stresses between Greenland and Newfoundland. None of these processes can operate in the mixed layer model due to the absence of ocean currents or the possibility of heat exchange with the deeper ocean. The absence of mixing with the deep ocean and the small vertical extension of the mixed layer is thought to be responsible for the much lower temperatures encountered south of Greenland in the MLO compared with the CGCM for positive NAO phases. The unrealistically shallow mixed layer of 50 m at high latitudes during winter [observed depths can reach up to several hundred meters according to Apel (1987, Fig. 2.4)] translates into a very small oceanic heat capacity of the MLO. In accordance with the concepts of Saravanan and McWilliams (1997) the consequences are reduced air–sea heat exchange due to strong negative feedbacks from the ocean and enhanced SST variance compared with the CGCM.

5. Stochastic forcing versus coupled modes

Up to this point the results presented have given evidence that even the low-frequency part (>10 yr) of atmospheric NAO variability is generated rather independently from the existence of a dynamical ocean. At first glance this does not seem to be in accordance with

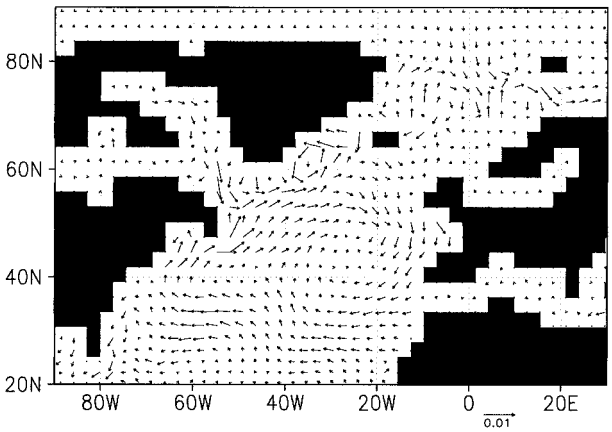

FIG. 7. As in Fig. 4a but for ocean surface velocity (m s^{-1}).

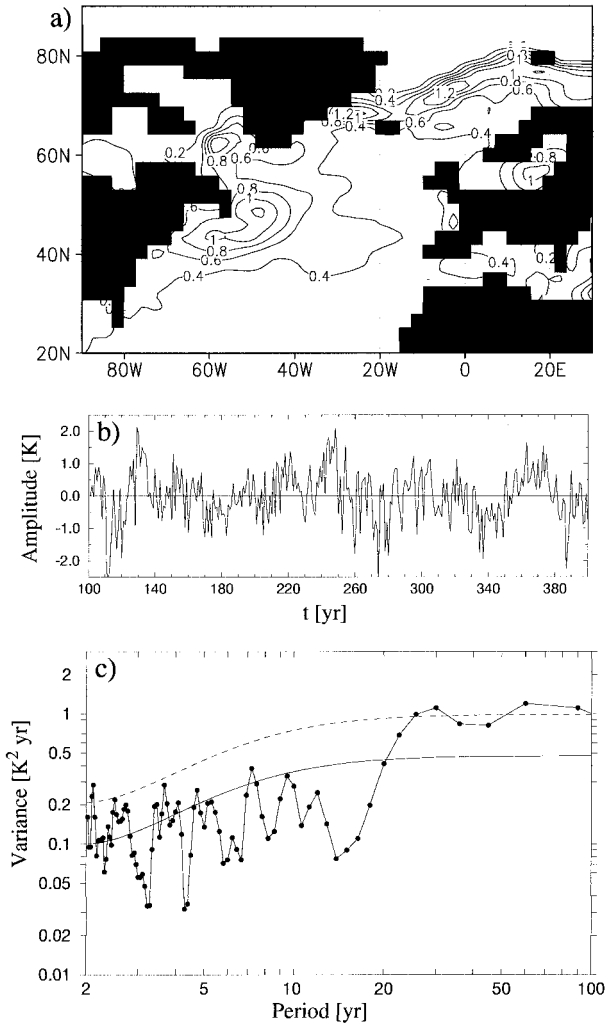

FIG. 8. (a) Geographical distribution of the standard deviation of unfiltered winter mean (Nov–Mar) SST anomalies (K) as simulated by the CGCM in the North Atlantic sector. Contour interval is 0.2. (b) Time series of unfiltered winter mean SST anomalies (K) averaged over the region 45°–50°W and 46°–51°N, located east of Newfoundland. (c) Power spectrum of winter mean SST anomalies averaged east of Newfoundland.

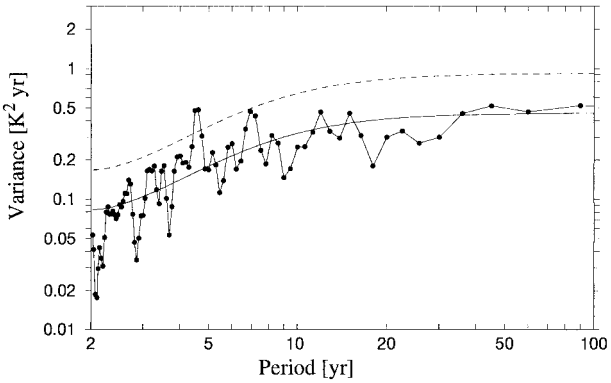

FIG. 9. Power spectrum of winter mean SST taken from the MLO and averaged south of Greenland (49°–56°W, 50°–57°N).

other studies searching for coupled atmosphere–ocean modes as the source of decadal and interdecadal NAO variability. In the following we will consider if there is evidence in our models for the existence of coupling mechanisms proposed in literature.

a. Ocean variability

Recent modeling results have given hints that the stochastic theory of Hasselmann (1976) may also be applicable at decadal and longer timescales (Manabe and Stouffer 1996). We investigate the SST variability produced in the model runs and, in particular, address the question if it is consistent with this theory. In the coupled run the standard deviation of the unfiltered winter mean fields of SST (Fig. 8a) displays an extended and highly active region to the east and southeast of Newfoundland where the Gulf Stream and the Labrador Current meet thereby producing a large meridional SST gradient. Note that the climatological position of this gradient is not exactly met by the model as it is unable to resolve the local system of ocean currents. The time series of SSTs averaged in the area of maximum variance (46°–51°N and 45°–50°W) is depicted in Fig. 8b. The corresponding energy spectrum in Fig. 8c essentially shows red noise characteristics with significant energy contributions (at the 95% confidence level above the red noise background) coming mainly from periods between 25 and 90 yr. This clearly demonstrates the existence of low-frequency variability in the western and central parts of the North Atlantic. Other centers of action, for example, in the Labrador, Iceland, and Greenland Sea, yield somewhat similar spectra. For these areas spectral peaks, however, are either not significant due to increased levels of red noise or shifted to periods greater than 90 yr.

A spectrum analysis of area-averaged SST of the MLO experiment taken from south of Greenland (50°–57°N, 49°–56°W) shows red noise behavior over the entire spectrum with no significant peak in the low-frequency part (Fig. 9). We conclude that the SST spectra in both models result mainly from the ocean integrating the atmospheric variability.

b. Coupling between atmosphere and ocean gyre circulation

As mentioned in the introduction, unstable air–sea interaction processes are thought to be one of the several possible explanations of decadal and interdecadal variability encountered both in the Pacific and in the North Atlantic. One approach involves the wind-driven gyre circulation (Latif and Barnett 1994; Grötzner et al. 1998).

One crucial element of the ''gyral mode'' is low-frequency variation of the wind stress curl coupling to the subtropical gyre. In the CGCM, a characteristic anomaly of the ocean surface currents is an intensified

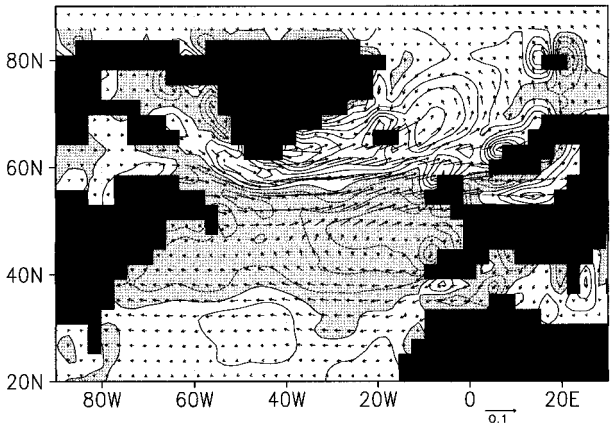

FIG. 10. As in Fig. 4a but for Ekman pumping (g m^{-2} s^{-1}) (displayed as contours) and wind stress (Pa) (displayed as vectors).

anticyclonic circulation between 25° and 55°N during a positive NAO phase (Fig. 7). The associated atmospheric forcing through wind stress (denoted by arrows) and the Ekman-induced vertical mass transport (denoted by contours) are plotted in Fig. 10. A strong negative anomaly located over the eastern parts of the North Atlantic between 35° and 55°N is indicative of anomalous Ekman pumping directed downward into the mixed layer, an effect arising from the equatorward (poleward) Ekman drift in the west wind (trade wind) zone and the resulting convergence of mass in the center of the gyre. Water masses are subducted equatorward with the mean horizontal circulation in the Sverdrup regime of the eastern and central Atlantic and balanced by an anomalously strong poleward-directed western boundary current. These processes are known to gradually spin up the entire subtropical gyre circulation. Therefore we expect the atmospheric forcing to lead the model's western boundary current by a few years due to the ocean's inertia.

This assumption is checked by correlating the decadal NAO index with the surface velocity of the ocean currents at each grid point. We found that the anomalous zonal velocity component is directed eastward in a region east of Newfoundland (30°–50°W) with an optimal lag of about 2–4 yr and westward in the subtropical East Atlantic with a lag of 1–3 yr (see Fig. 11a). The meridional velocity component is directed poleward in the northwest Atlantic (see Fig. 11b) with slightly longer lags involved of about 4–5 yr. This result is in fact indicative of an increasingly strengthened North Atlantic Current during a positive NAO phase, where the ocean takes several years to adjust to the imposed anticyclonic wind stress forcing.

A coupled climate system, however, consists of more than the causality relationship verified above, that is, forcing of the atmosphere and passive response of the ocean. It is the ocean feeding back onto the atmosphere that may result, under certain conditions, in a rather predictable linear oscillator of the two subsystems (Sar-

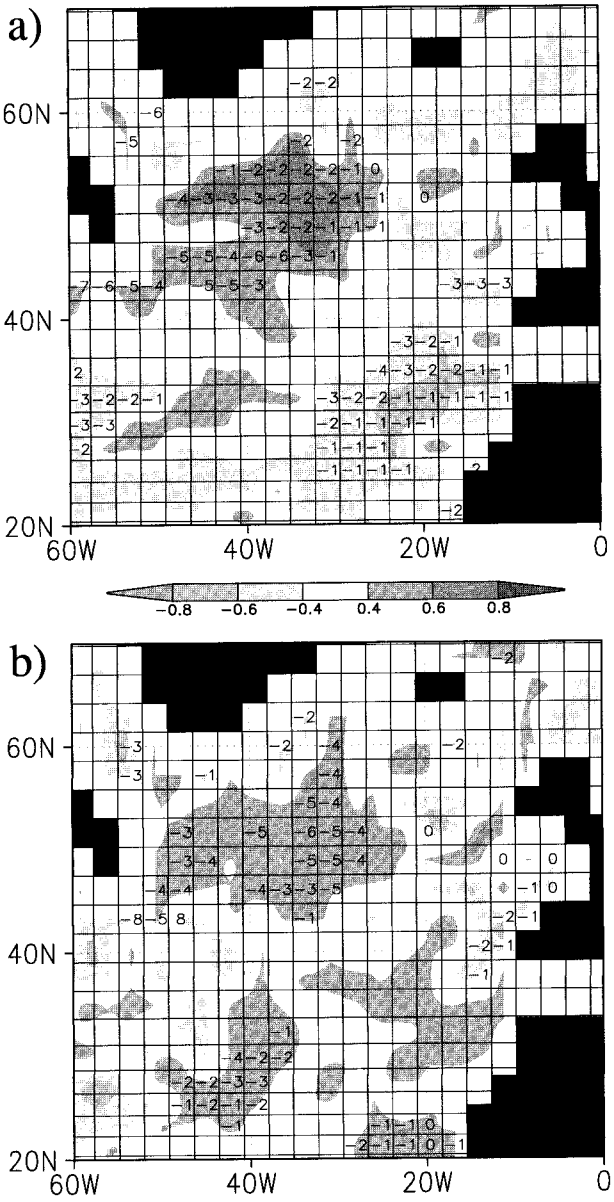

FIG. 11. Geographical distribution of CGCM cross-correlation coefficients between decadal NAO index and ocean surface velocity denoted by shading: (a) zonal component, (b) meridional component. Optimal lag for each grid box is marked by numbers (yr). Negative (positive) lags are indicative of the NAO leading (lagging behind) the surface velocities.

avanan and McWilliams 1998). The weak but rather defined spectral peak around 30 yr found both in the SST and SLP spectra of the CGCM strongly points in this direction. The feedback processes, however, are still not fully understood. It is believed that the anomalous northward flow of relatively warm waters in the northwestern Atlantic is directed across isotherms and thus acts to reduce the existing temperature gradient. This process could eventually contribute to the reversal of the formerly negative subpolar SST anomaly. Direct dia-

batic heating of the atmosphere or indirect effects via the atmospheric storm track could then trigger the phase reversal of the NAO. Thus we conclude that in this model there are strong hints for the existence of a coupled atmosphere–ocean gyre mode. The variance explained by this mode, however, is rather small.

c. Meridional overturning and the NAO

A second coupling mechanism that has been proposed to be important with respect to the generation of low-frequency variability in the atmosphere involves the density-driven thermohaline circulation (Delworth et al. 1993; Saravanan and McWilliams 1997; Timmermann et al. 1998). In particular, the decadal-scale NAO variability is suggested to be linked with the anomalous formation of bottom water at high latitudes (Delworth et al. 1993; Kushnir 1994; Griffies and Bryan 1997; Anderson et al. 1998; Latif 1998; Timmermann et al. 1998). Lag correlations between the NAO index and the MOT on the one hand and between the MOT index (time series taken at the climatological mean position of the overturning cell's center at 30°N and 2000-m depth) and SLP on the other hand were computed for the CGCM. Both approaches yield no significant signals. This result seems to be contradicting other modeling studies mentioned before. We hypothesize that in our model there could exist different ocean modes whose superposition may obscure the MOT signal during the NAO extreme phases. This will be investigated in more detail below.

In a few recent publications, the propagation of anomalies of certain quantities is mentioned to be involved in atmosphere–ocean coupling (Latif and Barnett 1994; Saravanan and McWilliams 1997; Grötzner et al. 1998; Timmermann et al. 1998). It turned out that in our models no such large-scale propagating features were present, which, however, does not a priori preclude the existence of coupled modes. Therefore an ordinary EOF analysis constitutes an appropriate tool for describing the leading low-frequency modes of the North Atlantic sector. The two dominant eigenmodes obtained explain together more than half of the domain's low-frequency fluctuations. The leading mode (Fig. 12a) is basin scale, has one polarity with largest loadings off the coast of Newfoundland, and explains ~43% of the variability. The corresponding PC is plotted in Fig. 12b. From regression analysis it turns out that the positive phase of this SST mode can be associated with the downwelling (see Fig. 13a) of relatively warm and saline surface waters (see Fig. 13b) in subpolar regions, largely around 70°N. No significant lags are involved in this process. When asking for the relationship of this mode with the atmosphere we find a weak association with a NAO-like mass distribution near the surface (Fig. 13c) and no significant freshwater flux anomalies in the Greenland–Iceland–Norwegian (GIN) Seas (no plot shown),

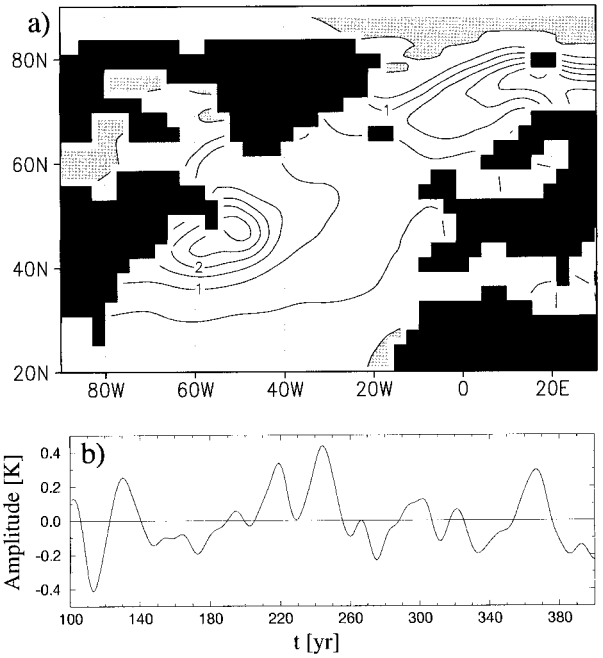

FIG. 12. (a) First EOF of North Atlantic SST anomalies based on 10-yr low-pass-filtered winter (Nov–Mar) means of the CGCM. Contour interval is 0.5 and negative values are shaded. This mode explains 43% of the low-frequency variance. (b) Time series of first principal component of SST (K).

which are the location of the model's major downwelling branch in the long-term mean (Zhang et al. 1998).

The second SST eigenmode accounts for ~15% of the variance and is characterized by a dipole pattern with one center of action located southeast of Newfoundland and centers of opposite sign in the Labrador and GIN Seas (Fig. 14a). The associated PC is depicted in Fig. 14b. At high latitudes a small meridional overturning cell can be associated with this SST configuration according to a regression analysis. The relationship is such that, for instance, an enhanced meridional temperature gradient in the North Atlantic is connected with a weakened downwelling around 70°N (Fig. 15a). The overlying atmosphere during this specific SST anomaly configuration exhibits a typical NAO pattern in SLP (Fig. 15b) with negative (positive) values in subpolar (subtropical) regions. Precipitation minus evaporation ($P - E$) possesses large positive values in the GIN Seas resulting in a major freshening of surface waters (Fig. 15c). Increased storm track activity [for definition see Christoph et al. (1995)] over the northeast Atlantic during positive NAO phases (see Fig. 16) is thought to contribute to these anomalous freshwater fluxes into the ocean through enhanced release of latent heat (Hoskins and Valdes 1990).

In short summary one could speculate that the existence of two major oceanic variability modes in the CGCM may not be a pure figment of the EOF analysis, but could be based on two different physical mecha-

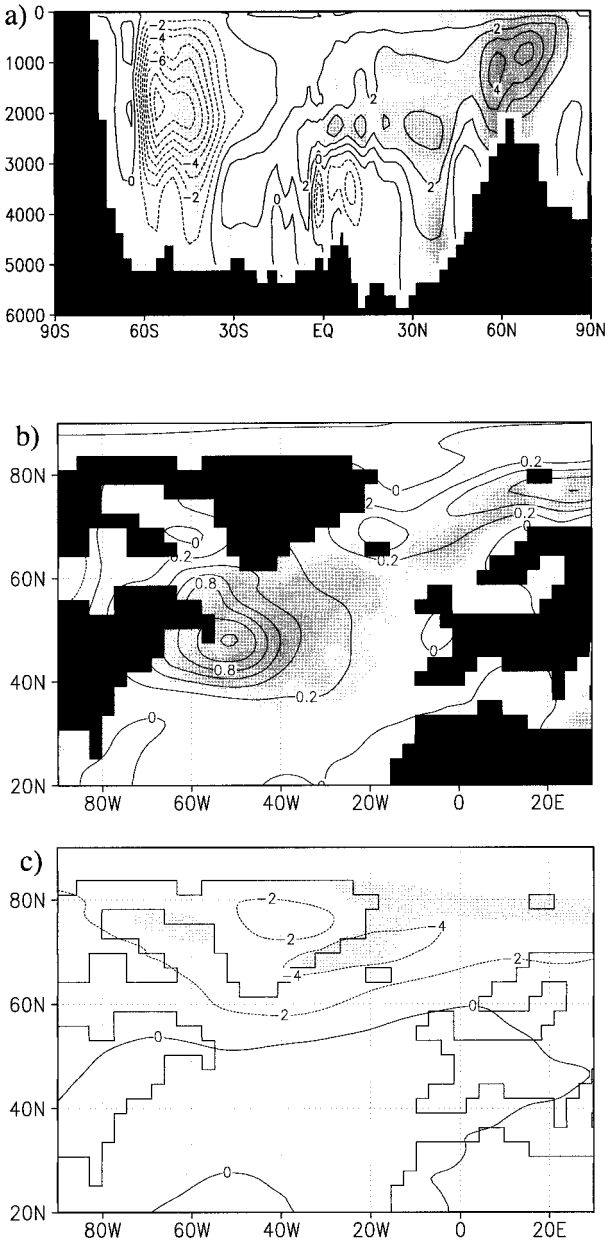

FIG. 13. First principal component of SST (cf. Fig. 12b) regressed upon 10-yr low-pass-filtered fields of (a) meridional overturning function in the Atlantic basin (contour interval is 1 Sv K^{-1}), (b) sea surface salinity (contour interval is 0.2 g kg^{-1} K^{-1}), and (c) sea level pressure (contour interval is 2 hPa K^{-1}). Shading from light to dark indicates explained variances by the linear regression model starting from 20% in steps of 10%.

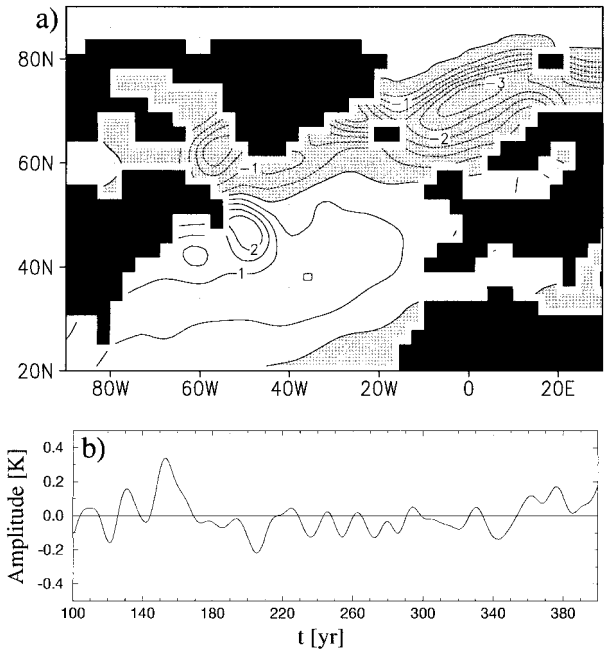

FIG. 14. (a) As in Fig. 12a but for the second EOF. This mode explains 15% of the low-frequency variance of CGCM's SST. (b) Time series of second principal component of SST (K).

nisms. On the one hand the NAO may determine the wind-driven advection of warm and saline surface waters from the subtropics by anomalous ocean currents into the subpolar sinking regions, thereby enhancing or suppressing the THC nonlocally. Additionally the THC could be forced by the anomalous export of sea ice driven by surface winds as suggested by Hilmer et al. (1998). On the other hand the NAO influences the freshwater fluxes in the GIN Seas via the storm track, thereby affecting the THC locally. Since both processes work in opposite directions, their superposition could be the reason for the lack of a MOT signal from the perspective of the atmosphere in the long-term mean. The preconditions, however, leading to one or the other mechanism are not clear and should be addressed in a separate study.

d. Coupling between atmosphere and cryosphere

A third self-sustaining process possibly operating in the model on decadal timescales involves high-latititude interactions between the atmosphere, the cryosphere, and most likely also the ocean. We find that in the coupled model sea-ice concentration and thickness are sensitive to decadal-scale NAO fluctuations in the Baffin Bay, in the northern parts of the Hudson Bay, in the Labrador Sea, and, with opposite sign, also in the Baltic Sea (not shown). We wanted to focus on the sensitive Arctic region (60°–70°N, 60°–80°W) and thus computed the area-averaged time series of sea-ice concentrations. Lag correlation analysis with the NAO index yields that low pressure over Greenland is followed by maximum sea-ice concentrations in the Baffin Bay area about 3 yr later (see Fig. 17a, solid line). In these Arctic regions the heat exchange between ocean and atmosphere is strongly controlled by the sea-ice distribution. Polynias and leads are known to be capable of effectively forcing the troposphere (Grötzner et al. 1994). It turns out that in the Baffin Bay upward-directed net surface heat flux leads lower than normal surface pressure by about 6 yr

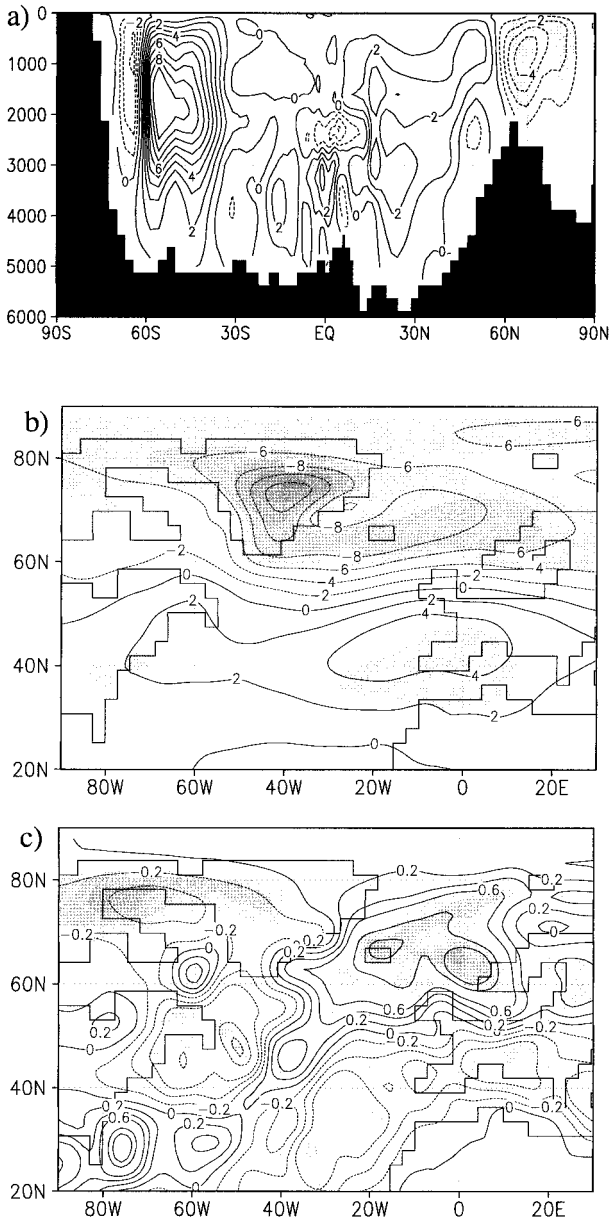

FIG. 15. (a) Second principal component of SST (cf. Fig. 14b) regressed upon 10-yr low-pass-filtered fields of (a) meridional overturning function in the Atlantic basin (contour interval is 1 Sv K^{-1}), (b) sea level pressure (contour interval is 2 hPa K^{-1}), and (c) precipitation–evaporation (contour interval is 0.2 mm d^{-1} K^{-1}). Shading from light to dark indicates explained variances by the linear regression model starting from 20% in steps of 10%.

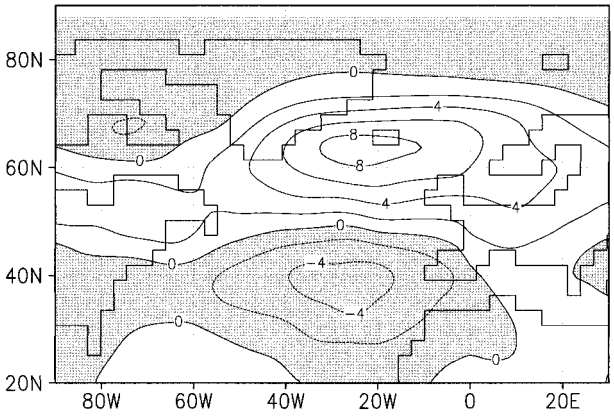

FIG. 16. As in Fig. 4a but for storm tracks (gpm).

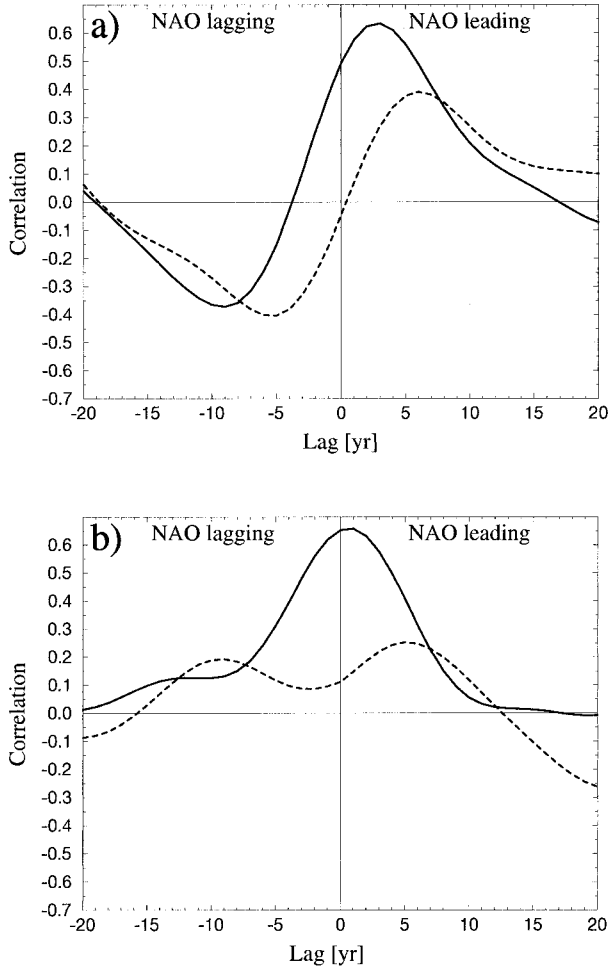

FIG. 17. Lagged cross correlations between decadal NAO index and the Baffin Bay area (60°–70°N, 60°–80°W) sea-ice concentrations (solid line) and the net surface heat flux (dashed line) as simulated by (a) the CGCM (T42) and (b) the MLO (T30).

and is also temporally 90° out of phase with the NAO index (see Fig. 17a, dashed line).

These findings could be consistent with a coupled mode as follows. Consider the time when the NAO index is zero, that is, when the SLP is in its climatological winter mean state most everywhere over the North Atlantic. In this case the model still possesses relatively low or high sea-ice concentrations and thicknesses west

of Greenland, depending on the sign of the NAO extreme a quarter of a cycle earlier. The absence of pressure anomalies is also linked with maximum upward- or downward-directed net surface heat flux anomalies only in that particular region. Although the spatial extent of this key area is rather limited, it could give an indication in which phase the NAO is going to swing next. The direct effect of diabatic heating (cooling) of the atmosphere could be the local formation of an initial surface low (high). For instance, low-level warming could labilize the entire tropospheric air column, which then enables the initial low to grow in height through enhanced vertical exchange. This might be one of the contributing factors for changing the large-scale circulation and thus eventually the sign of the NAO phase. While no long-term memory can be assigned to the sea ice itself, the memory of this coupled system could reside in the upper ocean's salinity profile. In periods of stronger than normal freezing in winter and subsequent melting in summer the salinity in the near-surface layers is lower than normal. This suppresses upward mixing of typically warm waters from the deeper ocean. The resulting high stability of the water column maintains a tendency to larger than normal sea-ice cover in the following years.

There exists, however, an alternative interpretation of the atmosphere–cryosphere relationship as well, where sea ice reacts merely passively to the NAO. Approximately 6 yr before a positive NAO maximum, the sea-ice concentrations are still low and heat fluxes into the atmosphere maximized while at a later stage the increasing sea-ice concentrations inhibit fluxes more strongly than reduced air temperatures enhance them. The sea-ice maximum occurs 3 yr after the temperature minimum is reached due to the retarding effect of vertical mixing in the upper ocean.

We can also check for possible interactions between the cryosphere and the atmosphere in the mixed layer ocean. Largely in accordance with the coupled model, sea-ice concentrations in the Baffin Bay/Labrador Sea are found to be sensitive to decadal-scale NAO. Time series of area-averaged (60°–70°N; 60°–80°W) sea-ice concentrations and net surface heat fluxes were formed and a lagged cross-correlation analysis performed. We find that sea ice is basically in phase with the NAO, with negative SLP anomalies over Iceland leading by 1 yr (Fig. 17b, solid line). The heat flux in that area (Fig. 17b, dashed line) shows no significant correlations with the NAO (threshold for 95% confidence level is $r = 0.3$). Thus, it seems that sea ice is playing a rather passive role in the mixed layer model.

6. Summary and conclusions

This paper deals with large-scale low-frequency fluctuations of the atmosphere in the extratropical North Atlantic region and their relation to the ocean. The role of ocean and sea-ice dynamics for these fluctuation is addressed by comparing two multicentury numerical simulations, one with a high-resolution (T42) coupled full ocean–atmosphere GCM (CGCM) and one with a coupled mixed layer ocean–atmosphere model (MLO) in T30. Except for spectral distributions 10-yr low-pass-filtered data are considered.

Atmospheric low-frequency variability is dominated by the NAO in both models. Regardless of the type of ocean underneath the atmosphere, the associated dipole patterns in SLP show general agreement regarding spatial distributions. Also variance and location of the two dipole centers are very close to observational estimates. The energy spectrum of the unfiltered NAO index time series of each model (based on the centers of strongest teleconnectivity) shows essentially white noise behavior at almost identical energy levels. A more objective measure of the NAO variability can be computed on the basis of the NAO's share of the domain's total low-frequency variability. According to EOF analyses of the SLP, this share is not significanly different in the two models. Total low-frequency SLP variance of the entire North Atlantic sector, however, is about 15% lower in the MLO with respect to the CGCM. This number translates directly into a 15% underestimation of NAO variability in the model without ocean dynamics.

The NAO-related variability pattern of SST exhibits a 10° northward shift in the CGCM with respect to the MLO. We assigned this shift of anomalies mainly to the existence of advection in the CGCM, which enables the anomalous northward transport of warm waters from the subtropics. Especially south of Greenland the amplitude of SST anomalies is much larger in the MLO than in the CGCM. This is the result of the limited damping effect of the fixed 50-m mixed layer (see also Saravanan and McWilliams 1997). In the CGCM the deeper ocean also contributes to the oceanic heat reservoir. The resulting much larger oceanic heat capacity increases the heat flux amplitudes by a maximum factor of four in the CGCM compared with the MLO. In contrast to the differences in SST anomaly distributions, the net surface heat flux patterns connected with the NAO show large spatial agreement in both simulations. This indicates that the locations of heat flux variability are directly connected to the atmospheric variability and are not significantly modified by the shift of the SST pattern.

Power spectra of unfiltered SST time series in dynamically active regions of the CGCM are characterized by essentially red noise behavior with superimposed peaks in the range of 30 yr and more. The spectral energy distribution of SST in the MLO is rather similar. There are, however, no significant peaks at longer timescales (>10 yr). This tells us that both simulations largely follow the stochastic climate model concept of Hasselmann (1976) and Frankignoul et al. (1997). The redness of the SST power spectra found represents the ocean's response to random white forcing of the atmosphere not only on interannual, but also on decadal

and longer timescales. Concerning the role of the ocean for low-frequency aspects of the NAO, a rather weak and statistically significant peak around 30 yr is noted in both SST and atmospheric spectra for the CGCM that is absent in the MLO. The presence of a rather well-defined and coherent timescale in each of the climate subsystems is considered indicative of the existence of coupled mechanisms.

Various concepts of coupled ocean–cryosphere–atmosphere modes associated with low-frequency variations of the NAO are suggested in literature. We tested for the existence of crucial elements of such modes in the CGCM. One concept of ocean–atmosphere coupling involves the wind-driven gyral circulation, as proposed by Grötzner et al. (1998). Our investigations confirmed that in fact low-frequency fluctuations of the wind stress curl associated with the NAO couple to the subtropical gyre in the CGCM, thereby spinning it up or down. It is, however, still not fully understood how the changed gyre circulation causes the NAO to eventually swing back in its opposite phase, that is, how the feedback loop is closed. Although hypotheses via direct or indirect diabatic heating at high latitudes and via the atmospheric storm track exist, quite a number of model experiments with prescribed forcing will have to be performed in the future in order to answer this question.

Another concept of ocean–atmosphere coupling involves the density-driven thermohaline circulation. We find no significant meridional overturning (MOT) associated with the NAO, which seems to be in contradiction with results recently reported by Timmermann et al. (1998). We hypothesize that both coupling processes are present in the model, but due to the superposition of countercurrent processes associated with the NAO in the GIN Seas (advection of dense surface waters versus local freshening of surface waters), the MOT signal is obscured when viewed from the atmosphere. Finally, from lag correlations we found hints for sea ice playing a potential role in the Baffin Bay area although a mere cause–effect interpretation is also conceivable.

Although we did not investigate the above-mentioned coupled modes in all depths, we nevertheless see strong indications for their existence. We conclude that these modes may be superimposed on a stochastically forced ocean, but contribute little additional variance to CGCM's atmosphere. Thus regarding the low-frequency variability of the NAO, the dynamic ocean does not seem to play a dominant role. Moreover, it is unclear if the underestimation of SLP variability in the MLO is really due to missing coupled modes involving ocean or ice dynamics. In fact, the 15% reduction of long-term variability could partly be due to the coarser horizontal resolution (T30) of the MLO run. Atmospheric Model Intercomparison Project–type experiments with this model yield also a very moderate reduction in variability over the North Atlantic with T30 compared with T42 (M. Stendel 1998, personal communication). Thus assigning the whole variability difference between the runs to the existence of coupled modes provides an upper boundary of their importance.

Even though it is not the focus of our study, we would like to mention the 7–8-yr peak, which occurs only in the observed atmosphere and in the CGCM. For the CGCM the missing of a corresponding signal in SSTs suggests that it is not indicative of a coupling mode. It may, however, hint at some limited predictive skill of the NAO on interannual timescales for reasons yet unknown. The question whether the occurrence of this spectral feature in the model is purely coincidental or based on the same physics as in reality deserves to be addressed in the near future.

In a recent study, Rodwell et al. (1999) reported that ensemble runs using observed SST were able to simulate the long-term NAO variability, at least for the second half of this century. This is, on the one hand, in contrast to our findings, which imply that the NAO has a rather chaotic nature, which, if reflecting the real climate, is discouraging in terms of the desire for long-term atmospheric predictions. On the other hand one has to take into account that the results presented here are based on the statistics of a relatively long integration. It may well be that the variance explained by coupled modes is more dominant for certain time periods und thus increase predictability. Also, we are aware that other GCMs may produce results different from ours. Certainly more model runs need to be analyzed in this respect in order to get more confidence.

Acknowledgments. This work has been supported by the German minister of research under Grant 07 VKV 01/1-25 and by the European Union under Grant ENV4-CT97-0499 (Project STOEC, Storm Track Upper Ocean Interactions and European Climate).

REFERENCES

Anderson, D., J. Marshall, and G. Komen, Eds., 1998: The role of the Atlantic in climate variability. Euroclivar/US Workshop Report, Florence, 56 pp. [Available from Euroclivar Office, P.O. Box 201, 3730 AE De Bilt, Netherlands.]

Apel, J. R., 1987: *Principles of Ocean Physics.* Academic Press, 634 pp.

Bacher, A., J. M. Oberhuber, and E. Roeckner, 1998: ENSO dynamics and seasonal cycle in the tropical Pacific as similated by ECHAM4/OPYC3 coupled general circulation model. *Climate Dyn.,* **14,** 431–450.

Barnett, T. P., 1983: Interaction of the Monsoon and the Pacific trade wind system at interannual timescales. Part I: The equatorial zone. *Mon. Wea. Rev.,* **111,** 756–773.

Bresch, D. N., and H. C. Davies, 1998: Sensitivity studies of NAO variability. *Proc. Ninth Conf. on Interaction of the Sea and Atmosphere,* Phoenix, AZ, Amer. Meteor. Soc., 65–68.

Christoph, M., U. Ulbrich, and U. Haak, 1995: Faster determination of the intraseasonal variability of storm tracks using Murakami's recursive filter. *Mon. Wea. Rev.,* **123,** 578–581.

CLIVAR, 1998: World Climate Research Programme Report No. 103, WMO/TD No. 869, 314 pp. [Available from International CLIVAR Project Office, Southampton Oceanography Centre, Empress Dock, Southampton SO14 3ZH, United Kingdom.]

Delworth, T., S. Manabe, and R. J. Stouffer, 1993: Interdecadal var-

iations of the thermohaline circulation in a coupled ocean–atmosphere model. *J. Climate,* **6,** 1993–2011.
Deser, C., and M. Blackmon, 1993: Surface climate variations over the North Atlantic Ocean during winter: 1900–1989. *J. Climate,* **6,** 1743–1753.
Ferranti, L., F. Molteni, and T. N. Palmer, 1994: Impact of localized tropical and extratropical SST anomalies in ensembles of seasonal GCM integrations. *Quart. J. Roy. Meteor. Soc.,* **120,** 1613–1645.
Frankignoul, C., P. Müller, and E. Zorita, 1997: A simple model of the decadal response of the ocean to stochastic wind forcing. *J. Phys. Oceanogr.,* **27,** 1533–1546.
Glowienka-Hense, R., 1990: The North Atlantic Oscillation in the Atlantic–European SLP. *Tellus,* **42A,** 497–507.
Griffies, S. M., and K. Bryan, 1997: A predictability study of simulated North Atlantic multidecadal variability. *Climate Dyn.,* **13,** 459–487.
Grötzner, A., R. Sausen, and M. Claussen, 1994: The impact of subgrid scale sea-ice inhomogeneities on the performance of the atmospheric general circulation model ECHAM3. *Climate Dyn.,* **12,** 477–496.
——, M. Latif, and T. P. Barnett, 1998: A decadal climate cycle in the North Atlantic Ocean as simulated by the ECHO coupled GCM. *J. Climate,* **11,** 831–847.
Halliwell, G. R., Jr., 1997: Decadal and multidecadal North Atlantic SST anomalies driven by standing and propagating basin-scale atmospheric anomalies. *J. Climate,* **10,** 2405–2411.
Hasselmann, K., 1976: Stochastic climate models. Part I: Theory. *Tellus,* **28,** 473–485.
Hilmer, M., M. Harder, and P. Lemke, 1998: Sea ice transport: A highly variable link between Arctic and North Atlantic. *Geophys. Res. Lett.,* **25,** 3359–3362.
Hoskins, B. J., and P. J. Valdes, 1990: On the existence of storm tracks. *J. Atmos. Sci.,* **47,** 1854–1864.
Hurrell, J. W., 1995: Decadal trends in the North Atlantic Oscillation and regional temperature and precipitation. *Science,* **269,** 676–679.
——, and H. van Loon, 1997: Decadal variations in climate associated with the North Atlantic Oscillation. *Climatic Change,* **36,** 301–326.
Kushnir, Y., 1994: Interdecadal variations in the North Atlantic sea surface temperature and associated atmospheric conditions. *J. Climate,* **7,** 141–157.
Kutzbach, J. E., 1967: Empirical eigenvectors of sea-level pressure, surface temperature and precipitation complexes over North America. *J. Appl. Meteor.,* **6,** 791–802.
Latif, M., 1998: Dynamics of interdecadal variability in coupled ocean–atmosphere models. *J. Climate,* **11,** 602–624.
——, and T. P. Barnett, 1994: Causes of decadal climate variability over the North Pacific and North America. *Science,* **266,** 634–637.
Manabe, S., and R. J. Stouffer, 1996: Low-frequency variability of surface air temperature in a 1000-year integration of a coupled atmosphere–ocean–land surface model. *J. Climate,* **9,** 376–393.
Mysak, L. A., D. K. Manak, and R. F. Marsden, 1990: Sea-ice anomalies observed in the Greenland and Labrador Seas during 1901–1984 and their relation to an interdecadal Arctic climate cycle. *Climate Dyn.,* **5,** 111–133.
Oberhuber, J. M., 1993a: Simulation of the Atlantic circulation with a coupled sea ice–mixed layer–isopycnal general circulation model. Part I: Model description. *J. Phys. Oceanogr.,* **23,** 808–829.
——, 1993b: The OPYC ocean general circulation model. Deutsches Klimarechenzentrum GmbH Tech. Rep. No. 7, 130 pp. [Available from Deutsches Klimarechenzentrum, Bundesstr. 55, 20146 Hamburg, Germany.]
Palmer, T. N., and Z. Sun, 1985: A modelling and observational study of the relationship between sea surface temperature in the northwest Atlantic and the atmospheric general circulation. *Quart. J. Roy. Meteor. Soc.,* **111,** 947–975.
Perlwitz, J., and H. F. Graf, 1995: The statistical connection between tropospheric and stratospheric circulation of the Northern Hemisphere in winter. *J. Climate,* **8,** 2281–2295.
Preisendorfer, R. W., 1988: *Principal Component Analysis in Meteorology and Oceanography.* C. D. Mobley, Ed., Elsevier, 425 pp.
Press, W. H., B. P. Flannery, S. A. Teukolsky, and W. T. Vetterling, 1989: *Numerical recipies.* Cambridge University Press, 702 pp.
Rodwell, M. J., D. P. Rowell, and C. K. Folland, 1999: Oceanic forcing of the wintertime North Atlantic Oscillation and European climate. *Nature,* **398,** 320–323.
Roeckner, E., and Coauthors, 1996: The atmospheric general circulation model ECHAM-4: Model description and simulation of present-day climate. Max Planck Institute Report No. 218, 90 pp. [Available from Max Planck Institute for Meteorology, Bundesstr. 55, 20146 Hamburg, Germany.]
Rogers, J. C., 1984: The association between the North Atlantic Oscillation and the Southern Oscillation in the Northern Hemisphere. *Mon. Wea. Rev.,* **112,** 1999–2015.
——, 1990: Low frequency monthly sea level pressure variability (1899–1986) and associated wave cyclone frequencies. *J. Climate,* **3,** 1364–1379.
——, 1997: On the cause of mild winters in northern Europe. NCAR Tech. Note NCAR/TN-433+PROC, 51–67. [Available from NCAR, P.O. Box 3000, Boulder, CO 80307.]
Saravanan, R., 1998: Atmospheric low frequency variability and its relationship to midlatitude SST variability: Studies using the NCAR climate system model. *J. Climate,* **11,** 1386–1404.
——, and J. C. McWilliams, 1997: Stochasticity and spatial resonance in interdecadal climate fluctuations. *J. Climate,* **10,** 2299–2320.
——, and ——, 1998: Advective ocean–atmosphere interaction: An analytical stochastic model with implications for decadal variability. *J. Climate,* **11,** 165–188.
Schmutz, C., and H. Wanner, 1998: Low frequency variability of atmospheric circulation over Europe between 1785 and 1994. *Erdkunde,* **52,** 81–94.
Stendel, M., and E. Roeckner, 1998: Impacts of horizontal resolution on simulated climate statistics in ECHAM4. Max Planck Institute Report No. 253, 57 pp. [Available from Max Planck Institute for Meteorology, Bundesstr. 55, 20146 Hamburg, Germany.]
Sutton, R. T., and M. R. Allen, 1997: Decadal predictability in North Atlantic sea surface temperature and climate. *Nature,* **388,** 563–567.
Timmermann, A., M. Latif, R. Voss, and A. Grötzner 1998: North Atlantic interdecadal variability: A coupled air–sea mode. *J. Climate,* **11,** 1906–1931.
Wallace, J. M., and D. S. Gutzler, 1981: Teleconnections in the geopotential height field during the Northern Hemisphere winter. *Mon. Wea. Rev.,* **109,** 784–812.
Wanner, H., R. Ricklim, E. Salvisberg, C. Schmutz, and M. Schüepp, 1997: Global climate change and variability and its influence on Alpine climate—Concepts and observations. *Theor. Appl. Climatol.,* **58,** 221–243.
Weare, B. C., and J. S. Nasstrom, 1982: Examples of extended empirical orthogonal function analysis. *Mon. Wea. Rev.,* **110,** 481–485.
Woods, J. D., 1985: The physics of thermocline ventilation. *Coupled Ocean–Atmosphere Models,* J. C. J. Nihoul, Ed., Elsevier Oceanography Series, Vol. 40, Elsevier, 543–590.
Yang, J., and J. D. Neelin, 1993: Sea–ice interactions with the thermohaline circulation. *Geophys. Res. Lett.,* **20,** 217–220.
Zhang, X.-H., J. M. Oberhuber, A. Bacher, and E. Roeckner, 1998: Interpretation of interbasin exchange in an isopycnal ocean model. *Climate Dyn.,* **14,** 725–740.